Van Vleck paramagnetism of chromium- and iron-doped II-VI semiconductors

E. Kartheuser
Institut de Physique, Université de Liège, B-4000 Liège 1, Belgium

Sergio Rodriguez
Department of Physics, Purdue University, West Lafayette, Indiana 47907-1396

Murielle Villeret
Department of Mathematics, City University, London EC1V 0HB, United Kingdom
(Received 3 May 1993)

We present a study of the Van Vleck paramagnets $A_{1-x}Cr_xB$ and $A_{1-x}Fe_xB$, where AB is a II-VI semiconductor having the zinc-blende or the wurtzite structure. In cubic zinc-blende hosts the nonlinear magnetization M depends on the orientation of the external magnetic field $\mathbf{B}$ with respect to the cubic axes of the crystal. We show that, while for iron M is largest when $\mathbf{B}$ is along a cubic axis and a minimum for $\mathbf{B}\|[111]$, for chromium the anisotropy is reversed and the largest value of M occurs for $\mathbf{B}\|[111]$. Expansions of the angular variation of the magnetization in terms of combinations of spherical harmonics invariant under the operations of the symmetry group (T_d or C_{3v}) of the site of the impurity are used to analyze the anisotropy. The magnetic-field dependence of the coefficients in the expansion is investigated. The magnetic susceptibility of Cr^{2+} in wurtzite-structure hosts is expected to be particularly large.

I. INTRODUCTION

A substance exhibits ordinary paramagnetism when the ground states of its atomic or molecular constituents possess permanent magnetic dipole moments, i.e., when their ground states have a degeneracy susceptible to being lifted under the influence of an external magnetic field. But, even when the lowest energy level of the components of the object of interest is nondegenerate, paramagnetic behavior still occurs as a consequence of mixing of higher multiplets into the ground state caused by the Zeeman interaction, $H_z=\mu_B(\mathbf{L}+g_e\mathbf{S})\cdot\mathbf{B}$. Here μ_B is the Bohr magneton, $\mathbf{L}$ and $\mathbf{S}$ the orbital and spin angular momentum operators of the individual components, g_e the g factor ($g_e\approx 2$) of the electron, and $\mathbf{B}$ the magnetic induction.

Even though this is a general phenomenon resulting from the failure of $\mathbf{L}+g_e\mathbf{S}$ to be a constant of the motion, it is often significant only when the ground state is nondegenerate, in which case the expectation values of $\mathbf{L}$ and $\mathbf{S}$ in zero magnetic field vanish in the ground state.[1] The resulting magnetism, characterized by a temperature-independent paramagnetic susceptibility near 0 K, was discussed by Van Vleck[2] in connection with the anomalous magnetic behavior of Eu^{3+} and Sm^{3+} in different salts and is appropriately called Van Vleck paramagnetism. The contribution to the magnetic moment per atom (or molecule) is

$$\mu(\hat{\mathbf{n}})=-\frac{\partial E^{(2)}}{\partial B}=2\mu_B^2 B\sum_{\nu}(E_\nu-E_0)^{-1}|\langle\nu|(\mathbf{L}+g_e\mathbf{S})\cdot\hat{\mathbf{n}}|0\rangle|^2 . \quad (1.1)$$

Here $E^{(2)}$ is the energy of the ground state as a function of $\mathbf{B}$ to second order in B, a typical stationary state of the system in the absence of an external magnetic field is denoted by $|\nu\rangle$ and the corresponding energy eigenvalue by E_ν, $\hat{\mathbf{n}}$ is a unit vector along the direction of the applied magnetic field, and the sum extends over all states except the ground state $|0\rangle$.

Equation (1.1) is only valid within the framework of second-order perturbation theory,[3] i.e., whenever

$$\mu_B|\langle\nu|(\mathbf{L}+g_e\mathbf{S})\cdot\hat{\mathbf{n}}|0\rangle|\ll E_\nu-E_0 . \quad (1.2)$$

The approximation (1.1) fails, therefore, when accessible low-energy excitations exist with energies comparable to or less than the magnitudes of the corresponding Zeeman interaction matrix elements. Then, one must develop alternative procedures to obtain the magnetization of the system. In this connection, several recent publications[4-17] have been concerned with the high-magnetic-field properties of iron ions at cation sites in cubic and wurtzite-structure II-VI semiconductors. Doubly ionized iron ions at cation sites in these materials have nondegenerate ground states resulting in Van Vleck paramagnetism.

In this paper we present a study of the magnetic properties of disordered, dilute alloys of the form $A_{1-x}C_xB(x\ll 1)$ where AB is a II-VI semiconductor, A being the cation and B the anion, and C is a magnetic ion. These alloys have recently received considerable attention and are called diluted magnetic semiconductors (DMS's).[18] In this work, we limit our discussion to DMS's in which the magnetic ion is either Fe^{2+} or Cr^{2+}.

The first few excited levels of Fe^{2+} in CdTe (site symmetry T_d) belong to the Γ_4, Γ_3, and Γ_5 irreducible repre-

0163-1829/93/48(19)/14127(8)/$06.00

sentations of T_d and lie about 20, 40, and 70 cm^{-1}, above the totally symmetric ground state,[7,19] respectively. Mixing of these levels into the Γ_1 ground state leads to a nonlinear magnetization M as a function of B which, because of the nature of the mixing, depends on the direction of $\mathbf{B}$ and, hence, gives rise to an anisotropy of M at large values of B. We shall show that in cubic zinc-blende hosts the anisotropy of the magnetization of chromium is opposite to that of iron. While for iron M is largest when $\mathbf{B}$ is along a cubic axis, for chromium the largest value of M occurs for $\mathbf{B}$ parallel to [111].

We express the magnetization in terms of the number p of effective Bohr magnetons per magnetic ion. The quantity p may be expanded in a series of even powers of the components of $\hat{\mathbf{n}}$ ($=\mathbf{B}/B$), each term of the series being an invariant with respect to all symmetry operations of the site group[20] (T_d). It is easy to show that the appropriate expansion is

$$p=p_0+p_4\left[Y_4^0(\theta,\phi)-\left[\frac{10}{7}\right]^{1/2}[Y_4^3(\theta,\phi)-Y_4^{-3}(\theta,\phi)]\right]$$
$$+p_6\left[Y_6^0(\theta,\phi)+\left[\frac{35}{96}\right]^{1/2}[Y_6^3(\theta,\phi)-Y_6^{-3}(\theta,\phi)]+\left[\frac{77}{192}\right]^{1/2}[Y_6^6(\theta,\phi)+Y_6^{-6}(\theta,\phi)]\right]+\cdots . \quad (1.3)$$

The combinations of spherical harmonics in Eq. (1.3) are obtained using functions belonging to the totally symmetric representation of T_d. Their averages over all directions of $\hat{\mathbf{n}}$ vanish.[21] The coefficients $p_0,p_4,p_6\ldots$ are functions of B and of the temperature T. The polar angle θ of $\hat{\mathbf{n}}$ is referred to the [111] direction as polar axis while the azimuth ϕ is measured from the $[11\bar{2}]$ direction. For low magnetic fields B, p_0 is linear in B while p_4 and p_6, initially, increase proportionally to the third and fifth powers of B, respectively.

In Sec. II we discuss the nature of the coefficients $p_0,p_4,p_6,\ldots$ for Cr^{2+} at Cd sites in CdTe and compare the results obtained with those for Fe^{2+} in CdTe.

The analysis of the magnetic properties of Fe^{2+} and Cr^{2+} at cation sites in II-VI semiconductors having the wurtzite structure, presented in Sec. III, is based, like that for cubic materials, on the crystal-field approximation but we assume that the crystal potential is tetrahedral to a high degree of approximation with a small trigonal distortion along the "cubic" body diagonal. The site symmetry of the magnetic ion is, therefore, C_{3v}. The appropriate expansion of the effective number of Bohr magnetons in this case is

$$p=p_0+p_2Y_2^0(\theta,\phi)+p_{40}Y_4^0(\theta,\phi)+p_{43}[Y_4^3(\theta,\phi)-Y_4^{-3}(\theta,\phi)]$$
$$+p_{60}Y_6^0(\theta,\phi)+p_{63}[Y_6^3(\theta,\phi)-Y_6^{-3}(\theta,\phi)]+p_{66}[Y_6^6(\theta,\phi)+Y_6^{-6}(\theta,\phi)]+\cdots . \quad (1.4)$$

Here the polar axis is the trigonal axis and ϕ is the angle $\hat{\mathbf{n}}$ makes with one of the σ_v mirror planes. In these materials, the Van Vleck magnetic susceptibility is anisotropic because the first two excited levels above the Γ_1 ground state have symmetries $\Gamma_2(C_{3v})$ and $\Gamma_3(C_{3v})$, the former lying below the latter. Since $(\mathbf{L}+g_e\mathbf{S})\cdot\hat{\mathbf{n}}$ only connects the Γ_1 ground state with Γ_2 states for $\hat{\mathbf{n}}$ parallel to the trigonal axis $\hat{\mathbf{c}}$, and to Γ_3 levels for $\hat{\mathbf{n}}$ perpendicular to $\hat{\mathbf{c}}$, the magnetic susceptibility, $\chi_\parallel$, for $\mathbf{B}$ parallel to $\hat{\mathbf{c}}$ exceeds $\chi_\perp$, the susceptibility for $\mathbf{B}$ perpendicular to $\hat{\mathbf{c}}$ [see Eq. (1.1)].

The calculations presented in this study make use of phenomenological crystal-field parameters derived from the rather extensive literature for iron-based DMS's. However, while there exist some optical absorption[22–24] and luminescence[25] studies of chromium-based DMS's, there is no published work on their magnetic properties. Thus, as we shall explain in Secs. II and III, we do not make use of the optical studies but estimate the parameters appropriate for these alloys by scaling those for Fe^{2+} in the same hosts.

II. MAGNETIC PROPERTIES OF CHROMIUM AND IRON IN CUBIC DILUTED MAGNETIC SEMICONDUCTORS

The macroscopic parameters $p_0,p_4,p_6,\ldots$ defined in Sec. I are related to the characteristic microscopic properties of the magnetic ion in the compound $A_{1-x}C_xB$. The potential at a cation site in a zinc-blende semiconductor can be written in the form

$$V=\frac{a'}{30}\sum[-(35\zeta^4-30\zeta^2r^2+3r^4)-20\sqrt{2}\zeta\xi(\xi^2-3\eta^2)] , \quad (2.1)$$

where the sum extends over all the electrons in the magnetic ion and ξ,η,ζ are the coordinates of a point measured from the center of the ion and referred to the $\hat{\xi},\hat{\eta},\hat{\zeta}$ axes parallel to $[11\bar{2}]$, $[\bar{1}10]$, and [111], respectively. The numerical coefficient a' can be estimated by calculating the electrostatic potential caused by the surrounding ions in the vicinity of the magnetic element. Assuming point

charged ions this estimate yields $a'=-(35ze^2/9R^5)$ where z is the effective anion charge and R the anion-cation distance. We do not follow this approach here but rather relate a' to a coefficient, denoted here by a, which appears as a prefactor of an operator equivalent to that in Eq. (2.1) when acting on states within a Russel-Saunders term (characterized by quantum numbers L and S) of the magnetic ion.[26] For a D term this potential is

$$V=-(a/30)[(35L_\xi^4-155L_\xi^2+72) +5\sqrt{2}\{L_+^3+L_-^3,L_\xi\}] . \quad (2.2)$$

Here $\mathbf{L}$ is the orbital angular momentum operator of the atom in units of $\hbar$, $L_\pm=L_\xi\pm iL_\eta$ and the curly brackets denote an anticommutator: $\{u,v\}=uv+vu$.

The parameter a can be related to a' and to $\langle r^4\rangle$, the average of the fourth power of the radial position of an electron over the $3d$ radial wave function of the magnetic ion. This relation is obtained making use of the Wigner-Eckart theorem and is written in the form[27]

$$a=a'\langle L\|\beta\|L\rangle\langle r^4\rangle$$

where $\langle L\|\beta\|L\rangle=\pm\frac{2}{63}$ for the ^5D terms of Fe^{2+} and of Cr^{2+} with the upper sign corresponding to Fe^{2+} and the lower one to Cr^{2+}. Since in a tetrahedral arrangement $a'<0$, $a<0$ for Fe^{2+} and $a>0$ for Cr^{2+}. In a tetrahedral field the orbital D term of a positively charged ion splits into a Γ_3 doublet and a Γ_5 triplet in which Γ_3 lies below Γ_5 for Fe^{2+} while the opposite occurs for Cr^{2+}. The energy level diagram shown in Fig. 1 illustrates both cases. It shows the orbital splitting in which the zero of energy is taken at the $^5\Gamma_3$ level [$\Delta=E(^5\Gamma_5)-E(^5\Gamma_3)=-6a$ is positive for Fe^{2+} and negative for Cr^{2+}]. The $^5\Gamma_3$ multiplet splits into five equidistant levels to second order in the spin-orbit interaction $\lambda\mathbf{L}\cdot\mathbf{S}$. The energies of these levels are $-24\lambda^2/\Delta, -18\lambda^2/\Delta, -12\lambda^2/\Delta, -6\lambda^2/\Delta$, and 0, their symmetry classifications being characterized by the $\Gamma_1,\Gamma_4,\Gamma_3,\Gamma_5$, and Γ_2 irreducible representations of T_d, respectively. The $^5\Gamma_5$ level splits into three levels of energies, $\Delta-2\lambda$, $\Delta+\lambda$, $\Delta+3\lambda$, with degeneracies 7, 5, and 3, respectively. To second order in λ these levels split further as indicated in Fig. 1 in the column labeled T_d. Thus the ground states of Fe^{2+} and Cr^{2+} in a tetrahedral environment are both singlets of symmetry Γ_1, the former originating from the orbital doublet Γ_3 and the latter from the Γ_5 triplet. The strength λ of the spin-orbit interaction is negative for Fe^{2+} (its value in CdTe, according to Udo *et al.*,[19] is -91 cm^{-1}) and positive for Cr^{2+} (in the present paper we take it equal to its free-ion value[28] 58 cm^{-1}). The last column, labeled C_{3v}, in Fig. 1 refers to the spectra of Fe^{2+} and Cr^{2+} in a wurtzite-structure DMS and is discussed in Sec. III.

The value of Δ, deduced from near-infrared-absorption data[19] is 2470 cm^{-1} for Fe^{2+} in CdTe. The corresponding quantity for Cr^{2+} in CeTe is

$$\Delta(Cr^{2+})=-\Delta(Fe^{2+})\langle r^4\rangle_{Cr^{2+}}/\langle r^4\rangle_{Fe^{2+}} =-3961.6\ \text{cm}^{-1}$$

obtained using the values[29] 4.496 and 7.211 atomic units for $\langle r^4\rangle$ in the $3d^n$ configurations of Fe^{2+} and Cr^{2+}, respectively.

The wave functions for the levels displayed in the column labeled T_d in Fig. 1 are given in Tables 6, 8, and 18 of Villeret, Rodriguez, and Kartheuser.[30] The magnetization is found forming the thermal average of the magnetic moments in the states obtained from the diagonalization of the Hamiltonian matrix of the ^5D term in the presence of an applied magnetic field. This program was carried out in Refs. 7 and 8 for Fe^{2+} in a cation site in a zinc-blende semiconductor.

For sufficiently large magnetic fields the magnetization of Fe^{2+} ions is anisotropic, as expected from the failure of second-order perturbation theory already mentioned in Sec. I. The magnetization is largest when $\mathbf{B}$ is directed along $\langle 001\rangle$ and is a minimum, for given $|\mathbf{B}|$, when $\mathbf{B}$ is parallel to $\langle 111\rangle$. The explanation of the result is as follows. In second-order perturbation theory the Zeeman energy mixes the Γ_1 ground state with the Γ_4 levels. However, if one wishes to obtain the energy eigenvalues to fourth powers in B, the Γ_4 level is mixed with Γ_3 for $\mathbf{B}$ along $\langle 001\rangle$ and with Γ_5 for $\mathbf{B}$ parallel to $\langle 111\rangle$. Since for Fe^{2+} in a T_d environment the Γ_3 level is below the Γ_5 level the admixture into Γ_1 of the former is larger when

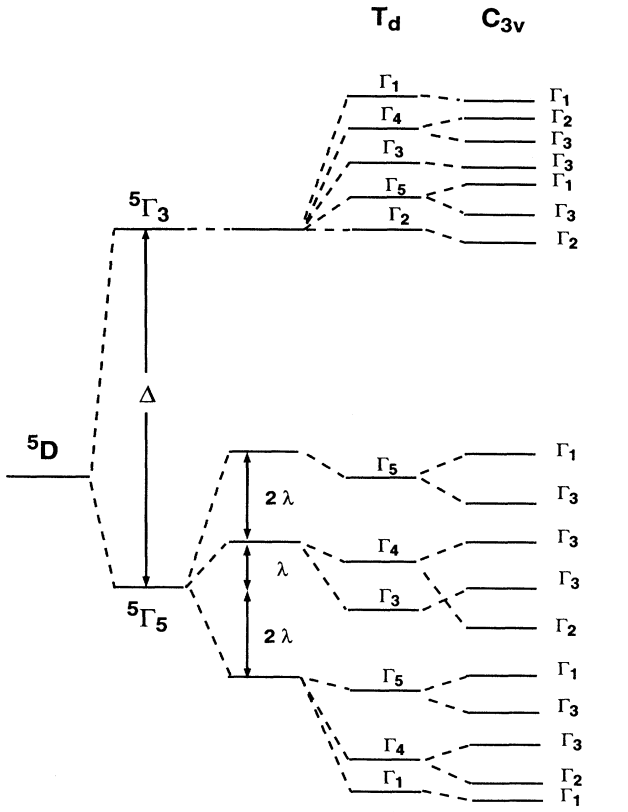

FIG. 1. Schematic drawing of the energy levels of Cr^{2+} and Fe^{2+} at a cation site in II-VI compounds having the zinc-blende (T_d) or the wurtzite (C_{3v}) structure. The group-theoretical notation follows that in Ref. 20. The zero of energy is selected at the $^5\Gamma_3$ orbital D state. For Cr^{2+}, $\Delta<0$ and $\lambda>0$. These signs are reversed for Fe^{2+}.

$\mathbf{B}\|[001]$ than that of the latter when $\mathbf{B}\|[111]$. Furthermore, the Γ_3 doublet splits significantly when $\mathbf{B}\|[001]$ while its degeneracy is not removed if $\mathbf{B}\|[111]$ (see Figs. 1, 2, and 6 in Ref. 7). Thus, the magnetic component of the perturbed ground state when $\mathbf{B}\|[001]$ is larger than that obtained when $\mathbf{B}\|[111]$, accounting for the observed result.

The situation in Cr^{2+} in a T_d environment is reversed. We note that the lowest Γ_5 level lies below the lowest Γ_3 level by, approximately, 3 times the strength of the spin-orbit interaction. Thus the contribution of mixing of Γ_5 into Γ_1 via Γ_4 exceeds that of Γ_3 into Γ_1 explaining the expected behavior described graphically in Fig. 2.

The results of calculations of the effective numbers of Bohr magnetons per Fe^{2+} and Cr^{2+} in CdTe at 4.2 K are shown in Fig. 2 where the features just mentioned are clearly displayed. As expected the saturation in the case of Cr^{2+} is reached at lower magnetic fields.

It is interesting to note that the saturation of p for large B is lower in $Cd_{1-x}Cr_xTe$ than in $Cd_{1-x}Fe_xTe$. In principle, at sufficiently large magnetic fields the saturation value of p for Fe^{2+} should be 4 if the Zeeman energy is small compared to Δ. The admixture of ${}^5\Gamma_5$ levels into the ${}^5\Gamma_3$ multiplet leads to a saturation value $p=4[1-(\lambda/\Delta)]\approx 4.6$. In Cr^{2+} only the lowest Γ_1, Γ_4, and Γ_5 states can contribute to the magnetic moment at even the largest available laboratory magnetic fields. Under this condition **L** and **S** are antiparallel and, thus, the saturation value of the magnetic moment equals three Bohr magnetons.

The magnetic susceptibilities of these ions in a T_d environment can be obtained by standard second-order degenerate perturbation theory; they are

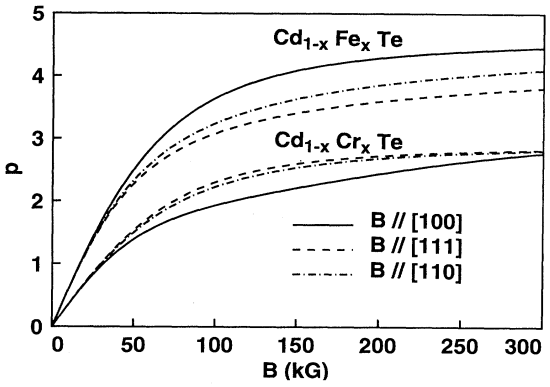

FIG. 2. Effective number of Bohr magnetons per magnetic ion in $Cd_{1-x}Fe_xTe$ and $Cd_{1-x}Cr_xTe$, at $T=4.2$ K for three orientations of the magnetic field with respect to the cubic axes of the crystal. The material parameters are $\Delta=2470\ cm^{-1}$ and $\lambda=-91\ cm^{-1}$ for $Cd_{1-x}Fe_xTe$ and $\Delta=-3961.6\ cm^{-1}$ and $\lambda=58\ cm^{-1}$ for $Cd_{1-x}Cr_xTe$.

$$\chi=\lim_{B\to 0}(np\mu_B/B)=(8n\mu_B^2\Delta/3\lambda^2)\left[1-\frac{4\lambda}{\Delta}\right]^2\left[1+\frac{5\lambda}{\Delta}\right]^{-1} \tag{2.3}$$

for Fe^{2+} and

$$\chi=\lim_{B\to 0}(np\mu_B/B)=-(2n\mu_B^2\Delta/3\lambda^2)\left[\left[1+\frac{4\lambda}{\Delta}\right]^2-\frac{8\lambda}{\Delta}\left[1+\frac{5\lambda}{\Delta}\right]^2\left[1-\frac{4\lambda}{\Delta}\right]^{-1}\right] \tag{2.4}$$

for Cr^{2+} where n is the number of magnetic atoms per unit volume. The corresponding susceptibilities are 0.335 and 0.201 cm^3/mol for Fe^{2+} and Cr^{2+} in CdTe, respectively.[31] Figure 3 shows the temperature dependence of the calculated magnetic susceptibilities for $Cd_{1-x}Fe_xTe$ and $Cd_{1-x}Cr_xTe$. Figures 4, 5, and 6 show the magnetic-field dependence of the Fourier coefficients p_0, p_4, and p_6, respectively, for Fe^{2+} and Cr^{2+} in CdTe.

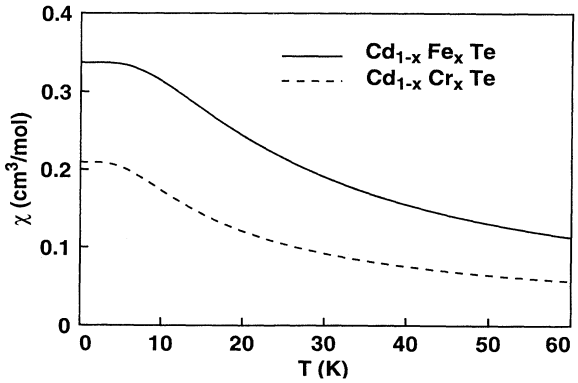

FIG. 3. Temperature dependence of the magnetic susceptibility of Fe^{2+} and Cr^{2+} in CdTe. Parameters as in Fig. 2.

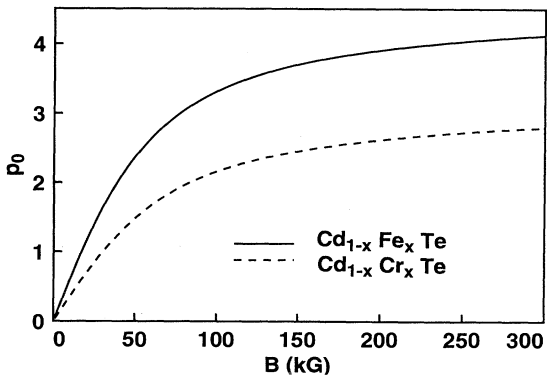

FIG. 4. Angular average p_0 of the effective number of Bohr magnetons of Cr^{2+} and Fe^{2+} in CdTe as a function of magnetic field. Temperature and material parameters as in Fig. 2.

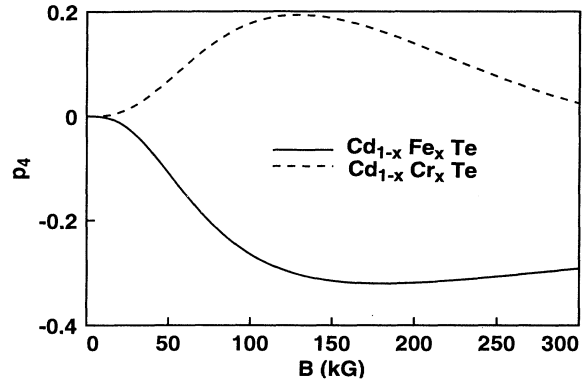

FIG. 5. Coefficient of the fourth-order cubic harmonic, p_4, in the expansion of p [Eq. (1.3)] as a function of magnetic field for Cr^{2+} and Fe^{2+} in CdTe. Note that the sign of the anisotropy of p is reflected in the different signs of p_4 for these two ions. Parameters as in Fig. 2.

The parameters used in this calculation are those already mentioned. The temperature is taken at 4.2 K. We note that while p_4 is negative for $Cd_{1-x}Fe_xTe$ it is positive for $Cd_{1-x}Cr_xTe$, which is consistent with the sign of the high-magnetic-field anisotropy of p exhibited by these alloys (see Fig. 2). The coefficients p_0, p_4, and p_6 were obtained calculating p for three inequivalent directions and solving the system of equations resulting from the substitution of the polar angles of these directions into the expansion (1.3).

III. MAGNETIC PROPERTIES OF CHROMIUM AND IRON IN WURTZITE-STRUCTURE SEMICONDUCTORS

The potential experienced by a magnetic ion at a cation site of a wurtzite-structure II-VI compound has, in addition to the tetrahedral contribution (2.1), a small trigonal field which we write in the form

$$V(C_{3v})=\frac{b'}{3}\sum(\xi^2+\eta^2-2\zeta^2)+\frac{c'}{60}\sum(35\zeta^4-30\zeta^2r^2+3r^4)\ , \tag{3.1}$$

where b' and c' measure the effect of the small trigonal distortion of the structure and, as in Eq. (2.1), the sums extend over all the electrons in the magnetic ion. We note that although $35\zeta^4-30\zeta^2r^2+3r^4$ and $\zeta\xi(\xi^2-3\eta^2)$ are invariant under the operations of C_{3v} (a subgroup of T_d where the $\hat{c}$ axis is parallel to [111]), we only include one of these terms to avoid redundancy. In fact, while for C_{3v} these invariants are independent, in T_d the only fourth degree invariant contains them in the combination shown in Eq. (2.1).

The operator equivalent associated with $V(C_{3v})$ is

$$V(C_{3v})=-b(2-L_\zeta^2)-(c/60)(35L_\zeta^4-155L_\zeta^2+72)\ , \tag{3.2}$$

where

$$b=b'\langle L\|\alpha\|L\rangle\langle r^2\rangle \tag{3.3}$$

and

$$c=c'\langle L\|\beta\|L\rangle\langle r^4\rangle\ . \tag{3.4}$$

For D terms[27] $\langle L\|\alpha\|L\rangle=\pm\frac{2}{21}$ where the positive (negative) sign corresponds to a less (more) than half-filled $3d$ shell. The values for $\langle L\|\beta\|L\rangle$ have been given in Sec. II.

According to Udo *et al.*,[19] $\Delta=2550.6$ cm^{-1}, $b=28.0$ cm^{-1}, and $c=-22.0$ cm^{-1} in $Cd_{1-x}Fe_xSe$. The corresponding values for $Cd_{1-x}Cr_xSe$ are $\Delta=-4091$ cm^{-1}, $b=-35.8$ cm^{-1}, and $c=35.3$ cm^{-1}, obtained from $b(Cr^{2+})=-b(Fe^{2+})\langle r^2\rangle_{Cr^{2+}}/\langle r^2\rangle_{Fe^{2+}}$ and $c(Cr^{2+})=-c(Fe^{2+})\langle r^4\rangle_{Cr^{2+}}/\langle r^4\rangle_{Fe^{2+}}$. The average $\langle r^2\rangle$ equals 1.781 a.u. for Cr^{2+} and 1.393 a.u. for Fe^{2+}. The splitting of the levels of Cr^{2+} and Fe^{2+} under the influence of the additional trigonal distortion (3.2) is shown in the right-hand column, labeled C_{3v}, of Fig. 1.

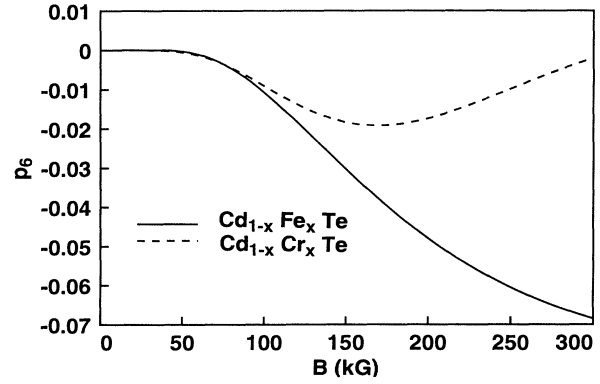

FIG. 6. Coefficient of the sixth-order cubic harmonic, p_6, in the expansion of p [Eq. (1.3)] as a function of magnetic field for Cr^{2+} and Fe^{2+} in CdTe. Temperature and parameters as in Fig. 2.

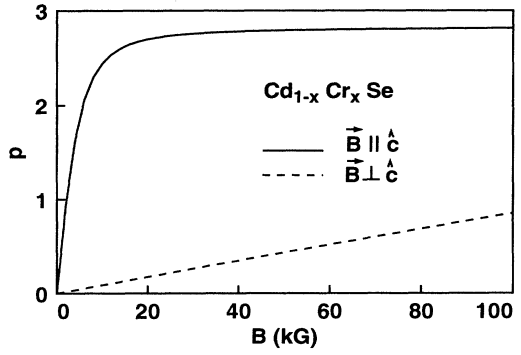

FIG. 7. Effective number of Bohr magnetons per ion in $Cd_{1-x}Cr_xSe$ as a function of the intensity of the magnetic field for **B** parallel to and perpendicular to the trigonal axis, $\hat{c}$. Parameters are $\Delta=-4091$ cm^{-1}, $\lambda=58$ cm^{-1}, $b=-35.8$ cm^{-1}, $c=35.3$ cm^{-1}; temperature $T=4.2$ K.

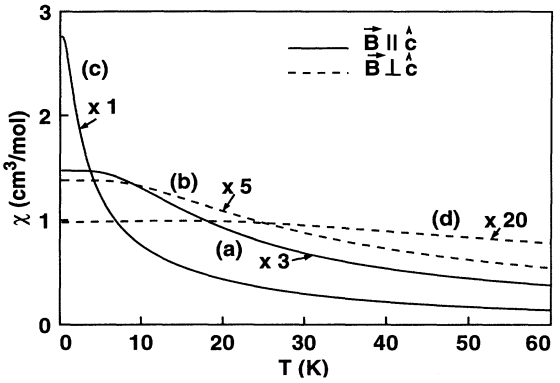

FIG. 8. Temperature dependence of the paramagnetic susceptibility of $Cd_{1-x}Fe_xSe$ [(a) and (b)] and of $Cd_{1-x}Cr_xSe$ [(c) and (d)] for **B** parallel to and perpendicular to the trigonal axis. Note that curves (a), (b), and (d) have been amplified by 3, 5, and 20, respectively. Parameters as in Fig. 7 for Cr^{2+}. For Fe^{2+}, $\Delta=2550.6$ cm^{-1}, $\lambda=-94.0$ cm^{-1}, $b=28.0$ cm^{-1}, and $c=-22.0$ cm^{-1}.

Figure 7 shows the calculated effective number of Bohr magnetons per Cr^{2+} ion in $Cd_{1-x}Cr_xSe$ at 4.2 K as a function of the intensity of the magnetic field **B** in either the direction of the trigonal axis or at right angles to it. We note the large anisotropy of the magnetic susceptibility. This is expected on the basis of the theory of the Van Vleck paramagnetism embodied in Eq. (1.1). In fact, the Zeeman interaction has nonvanishing elements only between Γ_1 and Γ_2 states if $\mathbf{B}\|\hat{\mathbf{c}}$ and only between Γ_1 and Γ_3 states when **B** is perpendicular to $\hat{\mathbf{c}}$. It turns out (as a result of numerical calculations) that in CdSe the lowest Γ_2 level of Cr^{2+} is considerably closer to the ground state than the lowest Γ_3 level.

Figure 8 shows the calculated temperature-dependence of the Van Vleck paramagnetic susceptibilities of Cr^{2+} and Fe^{2+} at cations sites in CdSe for **B** parallel to and perpendicular to the trigonal axis.

Figures 9–12 show the Fourier coefficients $p_0, p_2, p_{40}, p_{43}, p_{60}, p_{63}, p_{66}$ of the effective number of Bohr magnetons p for Cr^{2+} and Fe^{2+} in CdSe as functions of B. The numerical values of the coefficients were obtained at 4.2 K using the expansion in Eq. (1.4) and comparing it with the calculated values of p for **B** in seven independent orientations in the crystal. The coefficient p_2 reflects the anisotropy of the magnetic susceptibility of the system. Note that, as expected from the close proximity of the lowest Γ_2 level to the ground state of Cr^{2+} compared to that of Fe^{2+}, p_2 is larger in the former.

An interesting observation made in Refs. 12, 13, and 16 is that in $Cd_{1-x}Fe_xSe$ the p vs B curves cross at sufficiently high values of B. For small values of B, the effective number of Bohr magnetons for **B** along the trigonal axis $\hat{\mathbf{c}}$ is larger than p for $\mathbf{B}\perp\hat{\mathbf{c}}$ while for $B\approx 200$ kG this inequality is reversed by virtue of the anisotropy arising from the cubic contribution which is a minimum when $\mathbf{B}\|[111]$. Furthermore, the crossing of the p vs B curves occurs at different values of B depending on the direction of the magnetic field in the plane normal to $\hat{\mathbf{c}}$. In fact, the crossing occurs at lower magnetic fields when **B** lies in a σ_v plane of C_{3v} than when it is perpendicular to one of these planes.[16,32] These two directions in a

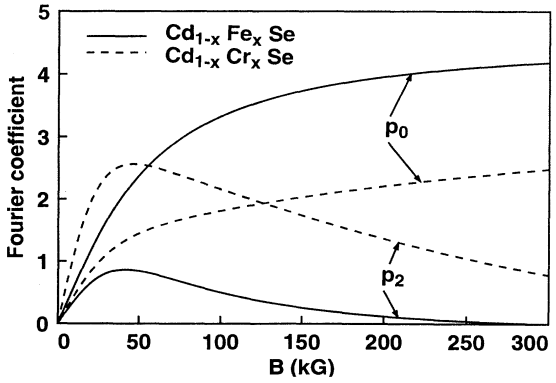

FIG. 9. Fourier coefficients p_0 and p_2 for the effective number of Bohr magnetons in $Cd_{1-x}Fe_xSe$ and $Cd_{1-x}Cr_xSe$ as a function of magnetic field. Parameters as in Fig. 8; temperature $T=4.2$ K.

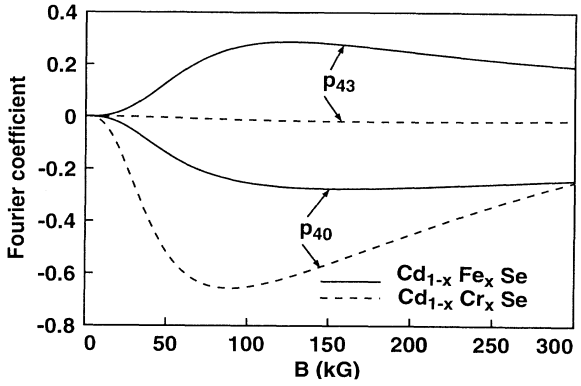

FIG. 10. Fourier coefficients p_{40} and p_{43}. Conditions and parameters as in Fig. 9.

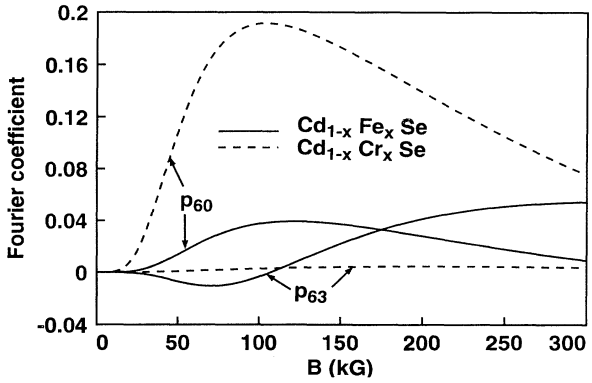

FIG. 11. Fourier coefficients p_{60} and p_{63}. Conditions and parameters as in Fig. 9.

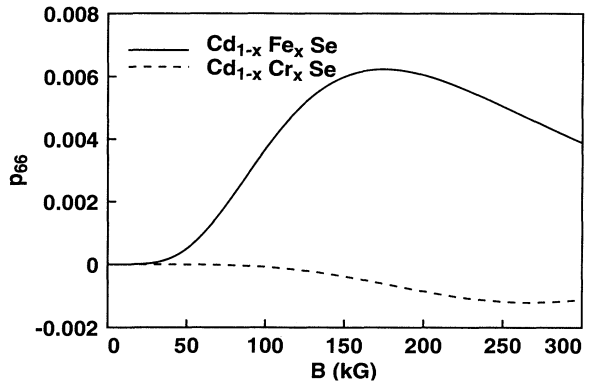

FIG. 12. Fourier coefficient p_{66}. Conditions and parameters as in Fig. 9.

plane normal to $\hat{\mathbf{c}}$ represent the extremes of this behavior.

It is interesting to note that the coefficient p_{66} in Eq. (1.4) is directly related to the anisotropy of p in the plane perpendicular to $\hat{\mathbf{c}}$. Indeed, we find that the difference between $p(\mathbf{B}\perp\sigma_v)=p(\mathbf{B},\theta=\pi/2,\phi=0)$ and $p(\mathbf{B}\|\sigma_v)=p(\mathbf{B},\theta=\pi/2,\phi=\pi/2)$ is given by

$$\Delta p=p(\mathbf{B}\|\sigma_v)-p(\mathbf{B}\perp\sigma_v)=1.932p_{66}\ .$$

A numerical calculation for Fe^{2+} in CdSe, using the parameters obtained from the near infrared absorption data of Udo *et al.*,[19] shows that the p vs B curves cross at $B_{CR}=199$ kG for $\mathbf{B}\perp\hat{\mathbf{c}}$ in a σ_v plane and at $B_{CR}=205$ kG for $\mathbf{B}\perp\hat{\mathbf{c}}$ normal to σ_v at absolute zero temperature. The corresponding values at 4.2 K are 201 and 207 kG, respectively. Thus, the change in B_{CR} as $\mathbf{B}$ is rotated by 90° in the plane perpendicular to $\hat{\mathbf{c}}$ from a direction in σ_v to one normal to it is ~ 6 kG.

In chromium-based DMS's, this behavior is not expected except at presently unattainable magnetic fields because of the large anisotropy of the magnetic susceptibility on the one hand and the reversed anisotropy (with respect to iron-based DMS's) of the nonlinear magnetization in cubic fields on the other.

IV. CONCLUDING REMARKS

The Van Vleck paramagnets among the II-VI compounds doped with magnetic ions of the iron group are those containing Cr^{2+}, Fe^{2+}, and Ni^{2+}. In this paper we have studied the magnetic properties of Cr^{2+} and Fe^{2+} in DMS's. We have shown that the anisotropy of the magnetization at high magnetic fields has opposite signs in chromium- and iron-based DMS's. We have not discussed nickel in detail for the following reasons. The lowest-energy term of Ni^{2+} is ^3F which splits in a crystal field of tetrahedral symmetry into $^3\Gamma_4$, $^3\Gamma_5$, and $^3\Gamma_2$ orbital multiplets, $^3\Gamma_4$ being the lowest. This in turn is split by the spin-orbit interaction into Γ_1, Γ_4, Γ_3, and Γ_5 levels, listed here in order of increasing energy.[33] Thus, Ni^{2+} in DMS is a Van Vleck paramagnet. However, the energy separation between the Γ_1 and Γ_4 levels is of order $3|\lambda|/2$. But λ, the strength of the spin-orbit interaction equals -324 cm^{-1} so that $3|\lambda|2\approx 486$ cm^{-1}. This energy is large enough for the paramagnetic behavior of nickel-based DMS's to be less dramatic than in the cases considered in the present work.

ACKNOWLEDGMENTS

This work was supported in part by the U.S. National Science Foundation–Materials Research Group (Grant No. DMR-934574), by the North Atlantic Treaty Organization (Research Grant No. 890866), and by Fonds de la Recherche Fondamentale et Collective (Belgium, Grant No. 2.4515.90). One of us (M.V.) wishes to acknowledge a travel grant from the Royal Society of London (United Kingdom).

---

[1]If ψ is a nondegenerate eigenstate of the Hamiltonian of a quantum-mechanical system, $H\psi=E\psi$, and T is the time-reversal operator, then $T\psi=c\psi$ where $|c|=1$ and $\langle T\psi|\mathbf{L}|T\psi\rangle=-\langle\psi|\mathbf{L}|\psi\rangle=c^*c\langle\psi|\mathbf{L}|\psi\rangle=0$. The same argument shows that $\langle\psi|\mathbf{S}|\psi\rangle=0$ and hence $\langle\psi|\mathbf{L}+g_e\mathbf{S}|\psi\rangle=0$. In some cases, when each state of a multiplet is its own time-reversed conjugate, the same conclusion holds. An interesting example occurs in Fe^{2+} in a T_d environment. The ^5D term of Fe^{2+} splits into $^5\Gamma_3$ and $^5\Gamma_5$, the former being the orbital ground state. The two orbital Γ_3 states are their own time-reversed conjugates so that $\langle\mathbf{L}\rangle=0$. We say that the orbital angular momentum is quenched.

[2]See J. H. Van Vleck, *The Theory of Electric and Magnetic Susceptibilities* (Oxford University Press, London, 1932).

[3]We note that in the sum over ν, we need only consider states whose symmetry properties permit the matrix elements of $(\mathbf{L}+g_e\mathbf{S})\cdot\hat{\mathbf{n}}$ to be nonvanishing.

[4]A. Twardowski, M. von Ortenberg, and M. Demianiuk, J. Cryst. Growth **72**, 701 (1985).

[5]C. Testelin, A. Mauger, C. Rigaux, M. Guillot, and A. Mycielski, Solid State Commun. **71**, 923 (1989).

[6]M. Villeret, S. Rodriguez, and E. Kartheuser, Solid State Commun. **75**, 21 (1990).

[7]M. Villeret, S. Rodriguez, and E. Kartheuser, Phys. Rev. B **43**, 3443 (1991).

[8]M. Villeret, S. Rodriguez, E. Kartheuser, A. Camacho, and L. Quiroga, Phys. Rev. B **44**, 399 (1991).

[9]S. Rodriguez, M. Villeret, and E. Kartheuser, Phys. Scr. **T39**, 131 (1991).

[10]C. Testelin, C. Rigaux, A. Mauger, A. Mycielski, and M. Guillot, Phys. Rev. B **46**, 2193 (1992).

[11]A. Twardowski, Solid State Commun. **68**, 1069 (1988).

[12]D. Scalbert, M. Guillot, A. Mauger, J. A. Gaj, J. Cernogora, C. Benoit à la Guillaume, and A. Mycielski, Solid State Commun. **76**, 977 (1990).

[13]T. Q. Vu, V. Bindilatti, M. V. Kurik, Y. Shapira, A. Twar-

dowski, E. J. McNiff, Jr., R. Kershaw, K. Dwight, and A. Wold, Solid State Commun. **76**, 605 (1990).

[14]A. Twardowski, K. Pakula, I. Perez, P. Wise, and J. E. Crow, Phys. Rev. B **42**, 7567 (1990).

[15]T. Q. Vu, V. Bindilatti, Y. Shapira, A. Twardowski, M. Demianiuk, and E. J. McNiff, Jr., Solid State Commun. **81**, 583 (1992).

[16]E. Kartheuser, S. Rodriguez, and M. Villeret, Solid State Commun. **84**, 635 (1992).

[17]Z. Wilamowski, H. Przybylinska, W. Joss, and M. Guillot, Semicond. Sci. Technol. **8**, S44 (1993).

[18]See, for example, *Diluted Magnetic Semiconductors*, edited by J. K. Furdyna and J. Kossut, Semiconductors and Semimetals (Academic, Boston, 1988), Vol. 25.

[19]M. K. Udo, M. Villeret, I. Miotkowski, A. J. Mayur, A. K. Ramdas, and S. Rodriguez, Phys. Rev. B **46**, 7459 (1992).

[20]The group-theoretical notation used in this work follows that of G. F. Koster, J. O. Dimmock, R. G. Wheeler, and H. Statz, *Properties of the Thirty-Two Point Groups* (MIT Press, Cambridge, MA, 1966).

[21]The coefficient of p_4 in Eq. (1.3) equals $(45/4\pi^{1/2})(n_y^2n_z^2+n_z^2n_x^2+n_x^2n_y^2-\frac{1}{5})$ where n_x,n_y,n_z are the direction cosines of **B** with respect to the cubic axes. It is a minimum along [001] and a maximum when $\hat{\mathbf{n}}\|[111]$, the corresponding numerical values being $-(9/4\pi^{1/2})$ and $(3/2\pi^{1/2})$, respectively. The coefficient of p_6 equals

$$\tfrac{9}{64}(13/\pi)^{1/2}[231n_x^2n_y^2n_z^2+2-21(n_y^2n_z^2+n_z^2n_x^2+n_x^2n_y^2)]$$

whose values are $\frac{9}{32}(13/\pi)^{1/2}$ and $\frac{1}{2}(13/\pi)^{1/2}$ for $\hat{\mathbf{n}}$ parallel to [001] and [111], respectively.

[22]J. T. Vallin, G. A. Slack, S. Roberts, and A. E. Hughes, Phys. Rev. B **2**, 4313 (1970).

[23]J. M. Langer and J. M. Baranowski, Phys. Status Solidi B **44**, 155 (1971).

[24]P. A. Slodowy and J. M. Baranowski, Phys. Status Solidi B **49**, 499 (1972).

[25]G. Grebe and H. J. Schultz, Z. Naturforsch. Teil A **29**, 1803 (1974).

[26]This procedure is called the method of operator equivalents. It was first developed by Stevens. See K. W. H. Stevens, Proc. Phys. Soc. London **65**, 209 (1952).

[27]See, for example, A. Abragam and B. Bleaney, *Electron Paramagnetic Resonance of Transition Ions* (Oxford University Press, London, 1970), pp. 670–676 and Table 19, p. 873.

[28]A. Abragam and B. Bleany, *Electron Paramagnetic Resonance of Transition Ions* (Ref. 27), p. 399.

[29]G. Burns, Phys. Rev. **128**, 2121 (1962); and *Electron Paramagnetic Resonance of Transition Ions* (Ref. 27), p. 399.

[30]M. Villeret, S. Rodriguez, and E. Kartheuser, Physica B **162**, 89 (1990). See correction in footnote 6 of M. Villeret, S. Rodriguez, and E. Kartheuser, Phys. Rev. B **47**, 1228 (1993). Tables 6 and 8 give the functions in terms of eigenvectors of L_z and S_z where z is one of the cubic axes. They can also be expressed in terms of the components of **L** and **S** with respect to $\hat{\xi}$, $\hat{\eta}$, and $\hat{\zeta}$. The appropriate functions for the $^5\Gamma_3$ states are listed in Table 18. Those for $^5\Gamma_5$ can be found in M. Villeret, Ph.D. thesis, Purdue University, 1989.

[31]The values quoted are per mole of magnetic component.

[32]A discussion of this effect is presented in Ref. 16, where Table I gives detailed numerical results for $Cd_{1-x}Fe_xSe$.

[33]M. Villeret, S. Rodriguez, and E. Kartheuser, Phys. Rev. B **41**, 10 028 (1990).